Robotica (2000) volume 18, pp. 213–217. Printed in the United Kingdom © 2000 Cambridge University Press

Iterative learning in variable structure position/force hybrid control of manipulators

Abílio Azenha

Department of Electrical and Computer Engineering, Faculty of Engineering, University of Porto, Rua dos Bragas, 4099 Porto Codex (Portugal)
e-mail: abilio_azenha@hotmail.com

(Received in Final Form: July 23, 1999)

SUMMARY
This paper presents a novel approach to the hybrid position/force control of robot manipulators employed in executing repetitive tasks that involve contact with the environment. The constraint surface is assumed to be a plane and its respective dynamics is modelled by a mass-dashpot-spring scheme. Time results obtained by simulations are very encouraging for future research and developments, because the system's behaviour is very efficient.

KEYWORDS: Iterative learning control; Position/force control; Variable structure control; Simulation; Environment modelling.

1. INTRODUCTION

With an increasing computing power at the present rate, one is faced with the possibility of developing simulation packages that employ that resource in a reasonable way. That is, one can use computers to predict the system's response even if they are very complex and computationally demanding. Following this line of thought, once the modelling and the simulation program are correct, one can derive important conclusions about the system's behaviour and performance without having to build or acquire an actual physical system.

On the other hand, iterative learning control (ILC) has been employed in recent years to improve the performance of robotic systems[1,2] or other general physical structures[3,4]. In this paper we developed a hybrid position/force ILC of robot manipulators and with variable structure controllers (VSCs)[5,6] in the control loops. The first work on hybrid position/force control of robot manipulators was due to Raibert and Craig[7]. Since then several researchers[8–16] increased the performance of their algorithm and studied the stability behaviour over all the workspace, including singular points neighbourhood.

The force control of robot manipulators can be classified into two main types: hybrid position/force control and impedance control. The first category is explained in this paper and it consists of selecting Cartesian directions that are position-controlled or force-controlled, since one cannot control the same direction in position and force at the same time. Impedance control[11] is aimed to establish a desired relationship between the position of the robot end-effector and the force exerted by the environment in terms of a differential equation. In this work the constraint surface is modelled by a linear model mass-dashpot-spring of lumped parameters and plane geometry is taken into account.

The paper is organised as follows. Section two introduces the ILC scheme to create the position/force hybrid algorithm presented in this paper. Section three shows some simulation results with ILCs and VSCs in terms of time responses. Finally, section four draws the main conclusions.

2. THE ITERATIVE LEARNING POSITION/FORCE HYBRID CONTROLLER

The dynamic equation of an ideal rigid-link-rigid-joint robot with n links interacting with the environment is:

$$\boldsymbol{\tau} = \mathbf{H}(\mathbf{q})\ddot{\mathbf{q}} + \mathbf{c}(\mathbf{q}, \dot{\mathbf{q}}) + \mathbf{g}(\mathbf{q}) - \mathbf{J}^T(\mathbf{q})\mathbf{F} \tag{1}$$

Here $\boldsymbol{\tau}$ is the $n \times 1$ vector of input torques, $\mathbf{q}$ is the $n \times 1$ vector of joint coordinates, $\mathbf{H}(\mathbf{q})$ is the $n \times n$ inertia matrix, $\mathbf{c}(\mathbf{q}, \dot{\mathbf{q}})$ is a $n \times 1$ vector of centrifugal/Coriolis terms and $\mathbf{g}(\mathbf{q})$ is the $n \times 1$ vector of gravitational effects. The $n \times m$ matrix $\mathbf{J}^T(\mathbf{q})$ is the transpose of the Jacobian matrix of the robot and $\mathbf{F}$ is the $m \times 1$ vector of the force that the (m-dimensional) environment exerts in the robot end-effector.

In this study it is adopted as prototype manipulator the 2R robot and a constraint plane determined by the angle θ depicted in Figure 1, with dynamics given by:

$$\mathbf{H}(\mathbf{q}) = \begin{bmatrix} (m_1+m_2)r_1^2 + m_2 r_2^2 & m_2 r_2^2 + m_2 r_1 r_2 C_2 \\ 2m_2 r_1 r_2 C_2 + J_{1m} + J_{1g} & \\ m_2 r_2^2 + m_2 r_1 r_2 C_2 & m_2 r_2^2 + J_{2m} + J_{2g} \end{bmatrix} \tag{2a}$$

$$\mathbf{c}(\mathbf{q}, \dot{\mathbf{q}}) = \begin{bmatrix} -m_2 r_1 r_2 S_2 \dot{q}_2^2 - 2m_2 r_1 r_2 S_2 \dot{q}_1 \dot{q}_2 \\ m_2 r_1 r_2 S_2 \dot{q}_1^2 \end{bmatrix} \tag{2b}$$

$$\mathbf{g}(\mathbf{q}) = \begin{bmatrix} g(m_1 r_1 C_1 + m_2 r_1 C_1 + m_2 r_2 C_{12}) \\ g m_2 r_2 C_{12} \end{bmatrix} \tag{2c}$$

$$\mathbf{J}^T(\mathbf{q}) = \begin{bmatrix} -r_1 S_1 - r_2 S_{12} & r_1 C_1 + r_2 C_{12} \\ -r_2 S_{12} & r_2 C_{12} \end{bmatrix} \tag{2d}$$

https://doi.org/10.1017/S026357479900199X Published online by Cambridge University Press

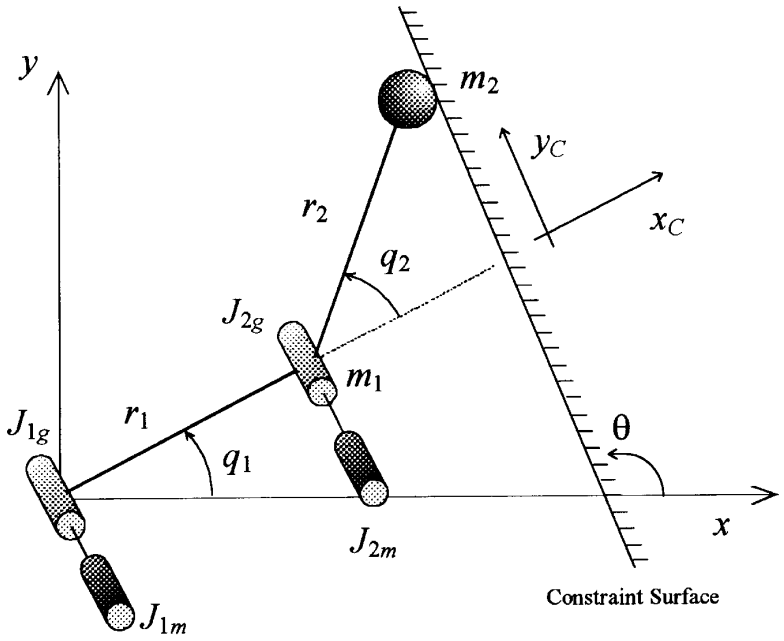


Fig. 1. The ideal 2R robot and the constraint surface.

where $C_i = \cos(q_i)$, $C_{ij} = \cos(q_i + q_j)$, $S_i = \sin(q_i)$ and $S_{ij} = \sin(q_i + q_j)$.

The numerical values adopted for the ideal 2R robot are enumerated in Table I.

Table I. The 2R robot parameters

i	m_i (Kg)	r_i (m)	J_{im} (Kgm^2)	J_{ig} (Kgm^2)
1	0.5	1.0	1.0	4.0
2	6.25	0.8	1.0	4.0

The contact of the robot with the constraint surface is modelled through a linear system with a mass M, a damping B and a stiffness K with dynamics:

$$F = M\ddot{x} + B\dot{x} + Kx \tag{3}$$

The schematic structure of the iterative learning position/force hybrid control algorithm is depicted in Figure 2. The diagonal matrix **S** is the $n \times n$ selection matrix with elements equal to one (zero) in the position(force) controlled directions and **I** is the $n \times n$ identity matrix. In this paper we consider the $y_C(x_C)$ Cartesian coordinates to be position

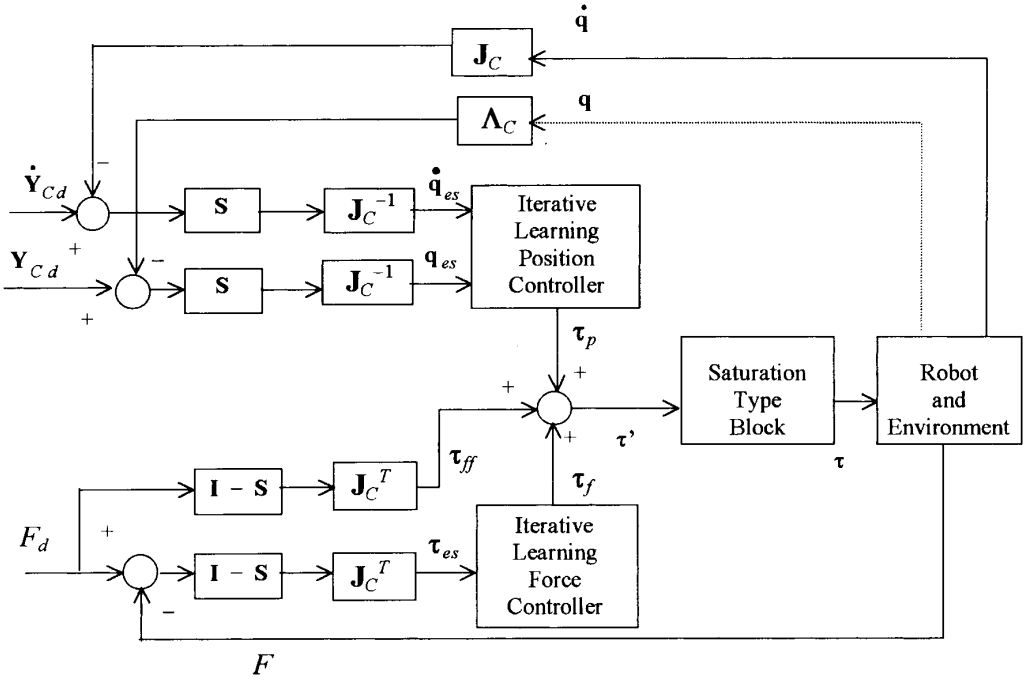


Fig. 2. Block diagram of the iterative learning position/force hybrid control algorithm.

https://doi.org/10.1017/S026357479900199X Published online by Cambridge University Press

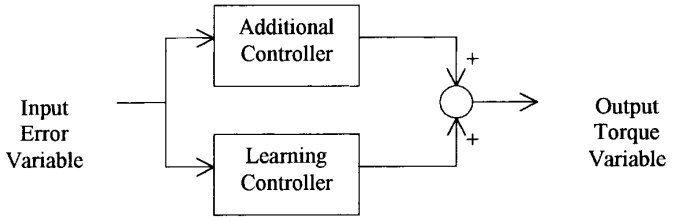


Fig. 3. Block diagram of the ILCs employed in this paper.

(force) controlled:

$$\mathbf{S}=\begin{bmatrix}0 & 0\\ 0 & 1\end{bmatrix} \tag{4a}$$

$$\mathbf{J}_C(\mathbf{q})=\begin{bmatrix}-r_1C_{\theta 1}-r_2C_{\theta 12} & -r_2C_{\theta 12}\\ r_1S_{\theta 1}+r_2S_{\theta 12} & r_2S_{\theta 12}\end{bmatrix} \tag{4b}$$

where $C_{\theta 1}=\cos(\theta-q_1)$, $C_{\theta 12}=\cos(\theta-q_1-q_2)$, $S_{\theta 1}=\sin(\theta-q_1)$ and $S_{\theta 12}=\sin(\theta-q_1-q_2)$.

The block diagram of the ILCs for the position and force loops is shown in Figure 3. The ILCs are defined in equations (5–6), and the additional controllers are chosen by the designer because they are dependent on the controlled system requirements.

The position ILC is specified by equations (5):

$$\tau_{pi}(k)=\tau_{pCONTRi}(k)+\tau_{plearni}(k) \tag{5a}$$

$$\tau_{plearni}(0)=0 \tag{5b}$$

$$e_{pi}(0)=0 \tag{5c}$$

$$e_{pi}(k)=q_{ei}(k) \tag{5d}$$

$$\tau_{plearni}(k)=\tau_{plearni}(k-1)+\beta_{posi}e_{pi}(k-1) \tag{5e}$$

where $i=1, 2$, k is the trial number, τ_{pCONTR} is the output of the additional position controller and β_{pos} is the position learning factor.

The force ILC is specified by equations (6):

Table II. Numerical values of the VSCs

Joint i	K_{Pi}	K_{Fi}	τ_{Pmaxi}	τ_{Fmaxi}
1	10^4	100	300	300
2	10^4	100	200	200

$$\tau_{fi}(k)=\tau_{fCONTRi}(k)+\tau_{flearni}(k) \tag{6a}$$

$$\tau_{flearni}(0)=0 \tag{6b}$$

$$e_{fi}(0)=0 \tag{6c}$$

$$e_{fi}(k)=\tau_{esi}(k) \tag{6d}$$

$$\tau_{flearni}(k)=\tau_{flearni}(k-1)+\beta_{fori}e_{fi}(k-1) \tag{6e}$$

where $i=1, 2$, k is the trial number, τ_{fCONTR} is the output of the additional force controller and β_{for} is the force learning factor.

The saturation type block is defined in equation (7):

$$\tau_i(k)=\begin{cases}\tau_{maxi} & ,\ \tau_i'(k)\geqslant\tau_{maxi}\\ \tau_i'(k) & ,\ |\tau_i'(k)|<\tau_{maxi}\\ -\tau_{maxi} & ,\ \tau_i'(k)\leqslant-\tau_{maxi}\end{cases} \tag{7}$$

where $i=1, 2$ and k is the trial number.

In the next section we present a simulation case study employing specific numeric values for the controllers parameters.

3. SIMULATION RESULTS

In this section we study the system response using VSCs, both at the position and force control loops and as additional controllers, with a sampling frequency of $f_c=1$ kHz. The constraint surface parameters are $M=0.03$ Kg, $B=1$ Ns/m and $K=400$ N/m, and the robot operating point is: $\theta=\pi/2$, $q_{10}=q_{20}=15\pi/36$. In this study, the position controller is the second-order VSC[5,6], in order to have small steady-state position errors, depicted in Figure 4. The parameters of the sliding surface are $\omega_{ni}=7.91$ rads^{-1} and $\xi_i=1.74$ ($i=1, 2$).

The force VSC is depicted in Figure 5. The parameters of

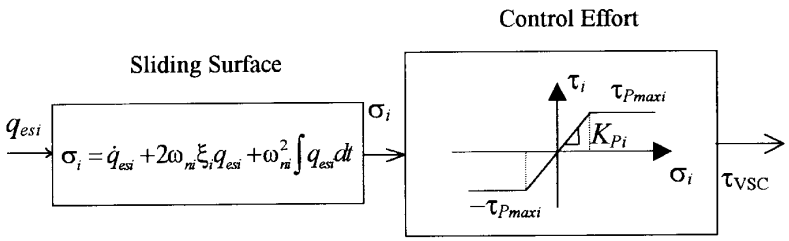


Fig. 4. Block diagram of the second order position VSC with integral action.

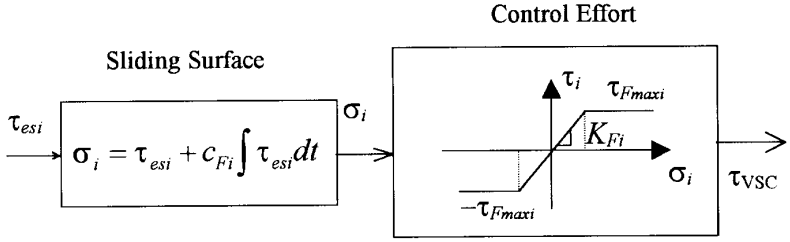


Fig. 5. Block diagram of the force VSC.

https://doi.org/10.1017/S026357479900199X Published online by Cambridge University Press

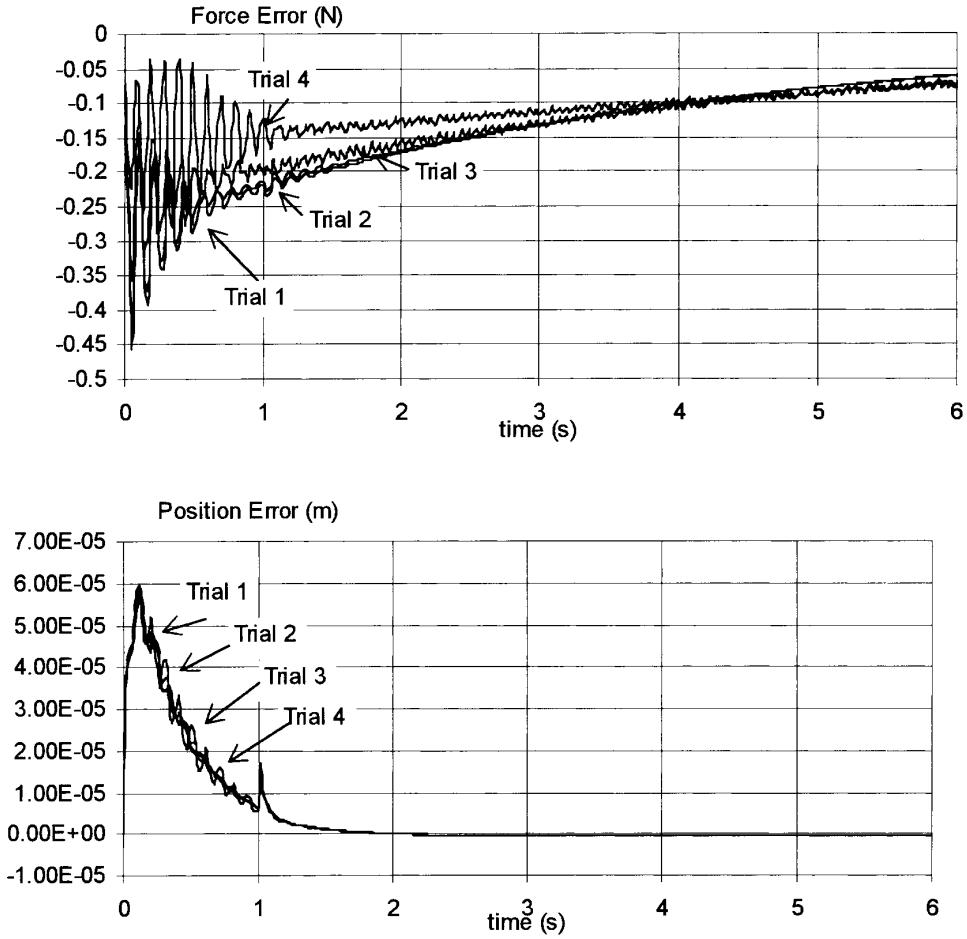


Fig. 6. Time responses of the simulated system (position and force errors).

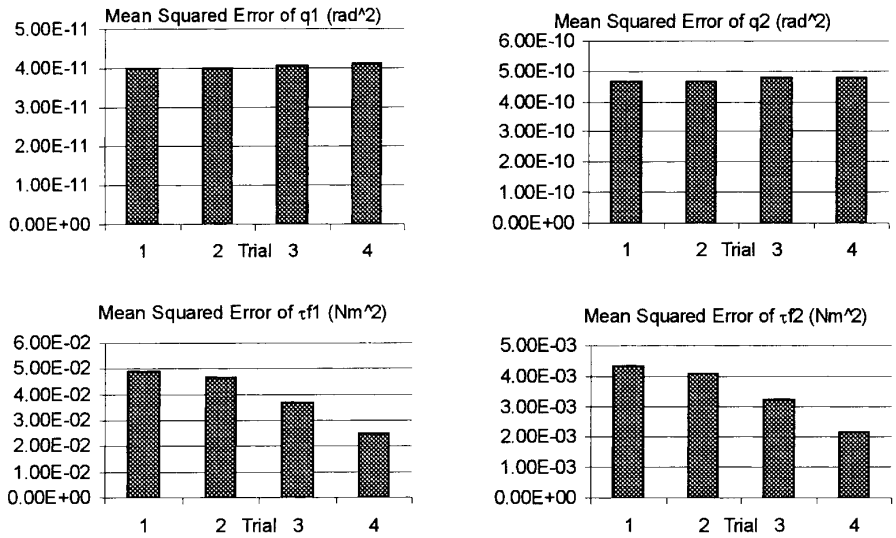


Fig. 7. Mean squared errors for the first four trials of the simulated system (position and force errors).

the sliding surface are $c_{Fi}=0.25\ \mathrm{s}^{-1}$ ($i=1, 2$).

Table II shows the numerical values of the control effort block adopted in this section.

The learning controller has the following parameters: $\beta_{posi}=0$, $\beta_{fori}=4$, $\tau_{maxi}=300$ Nm, $i=1, 2$. Increasing β_{posi} one obtains worse system responses. Figure 6 shows the time responses for the input signals $F_d=2t\ h(t) - 2(t-0.5)\ h(t-0.5)$ N and $y_{cd}=y_{c0}+0.01(t-1)\ h(t-1)$ m, where y_{c0} is the Cartesian position of the end-effector at $t=0$ s and $h(t)$ is the unit step. As the force error suggests, after the fourth trial one obtains more unstable responses, hence the solution is to stop the process of learning after that trial. Nevertheless, the system's performance is acceptable, because the position and force errors are very small.

The position and force mean squared errors are defined in expressions (8) and (9), respectively, $i=1,2$:

https://doi.org/10.1017/S026357479900199X Published online by Cambridge University Press

$$\frac{1}{T}\int_0^T q_{esi}^2(t)\,dt \tag{8}$$

$$\frac{1}{T}\int_0^T \tau_{esi}^2(t)\,dt \tag{9}$$

Figure 7 depicts the evolution of the mean squared errors for the first four trials.

In conclusion, the ILC system improves the force response after the first trial. The position error is negligible and is maintained nearly constant.

4. CONCLUSION

This paper presented an ILC scheme for the hybrid position/force algorithm of robot manipulators interacting with the environment and performing repetitive tasks. This strategy also employed VSCs in the position and force loops that were maintained, trial after trial. Time responses obtained through the system simulations showed the effectiveness of this learning algorithm, i.e, the position error is nearly constant and very small and the force error decreases with the trial number.

References

1. S.-M. Baek and T.-Y. Kuc, "An Adaptive PID Learning Control of DC Motors," in *Proceedings of the IEEE International Conference on Systems*, *Man*, *and Cybernetics*, Orlando, Florida, USA, (1997) pp. 2877–2882.
2. C.J. Chien, "A Discrete Iterative Learning Control for a Class of Nonlinear Time-Varying Systems," *IEEE Transactions on Automatic Control*, **43**, No 5, 748–752 (1998).
3. C.C. Cheah and D. Wang, "Learning Impedance Control for Robotic Manipulators," *IEEE Transactions on Robotics and Automation*, **14**, No 3 452–465 (1998).
4. H. Nishimura and K. Funaki, "Motion Control of Three-Link Brachiation Robot by Using Final-State Control with Error Learning," *IEEE/ASME Transactions on Mechatronics*, **3**, No 2 120–128 (1998).
5. A. Azenha and J.A.T. Machado, "Variable Structure Control of Systems with Nonlinear Friction and Dynamic Backlash," in *IFAC* 13*th World Congress*, San Francisco, California, USA, (1996). Vol. E, pp. 515–520
6. A. Azenha and J.A.T. Machado, "Dynamic Performance of Hybrid Robot Controllers Near Singularities," in *IEEE International Conference on Systems*, *Man*, *and Cybernetics*, La Jolla, San Diego, California, USA, (1998) pp. 3572–3577.
7. M.H. Raibert and J.J. Craig, "Hybrid Position/Force Control of Manipulators," *ASME Journal of Dynamic Systems*, *Measurement*, *and Control*, **102**, No. 2, 126–133 (1981).
8. M.T. Mason, "Compliance and Force Control for Computer Controlled Manipulators," *IEEE Transactions on Systems*, *Man, and Cybernetics*, **11**, No. 1, 418–432 (1981).
9. O. Khatib, "A Unified Approach for Motion and Force Control of Robot Manipulators: The Operational Space Formulation," *IEEE Journal of Robotics and Automation*, **3**, No. 1, 43–53 (1987).
10. D.E. Whitney, "Historical Perspective and State of the Art in Robot Force Control," *The Int. J. of Robotics Research*, **6**, No. 1, 3–14 (1987).
11. N. Hogan, "Impedance Control: An Approach to Manipulation, Parts I-Theory, II-Implementation and III-Applications," *ASME Journal of Dynamic Systems*, *Measurement*, *and Control*, **107**, No. 1, 1–24 (1985).
12. H. Zhang and R.P. Paul, "Hybrid Control of Robot Manipulators," *Proceedings of the IEEE International Conference on Robotics and Automation*, USA, (1985) pp. 602–607.
13. C.H. An and J.M. Hollerbach, "Kinematic Stability Issues in Force Control of Manipulators," *Proceedings of the IEEE International Conference on Robotics and Automation*, USA, (1987) pp. 897–903.
14. W.D. Fisher and M.S. Mujtaba, "Sufficient Stability Condition for Hybrid Position/Force Control," *Proceedings of the International Conference on Robotics and Automation*, Nice, France, (1992) pp. 1336–1341.
15. H. Bruyninckx and J. De Schutter, "Specification of Force-Controlled Actions in the "Task Frame Formalism"—A Synthesis," *IEEE Transactions on Robotics and Automation*, **12**, No. 4, 581–589 (1996).
16. B. Siciliano and L. Villani, "A Force/Position Regulator for Robot Manipulators Without Velocity Measurements," *IEEE International Conference on Robotics and Automation*, Minneapolis, USA, (1996) pp. 2567–2572.

https://doi.org/10.1017/S026357479900199X Published online by Cambridge University Press